Modeling Earth Systems and Environment (2024) 10:2221–2237
https://doi.org/10.1007/s40808-023-01899-9

ORIGINAL ARTICLE

Downscaling and reconstruction of high-resolution gridded rainfall data over India using deep learning-based generative adversarial network

Midhun Murukesh[1] · **Sreevathsa Golla**[1] · **Pankaj Kumar**[1]

Received: 18 February 2023 / Accepted: 5 November 2023 / Published online: 10 December 2023

Abstract
To expedite regional-scale climate change impact research and assessments, the downscaling of climate data is a crucial prerequisite. Image super-resolution, which is analogous to gridded data downscaling, is the concept of improving the pixel quality of images using deep learning techniques. In this study, the performance of a Super-Resolution Generative Adversarial Network (SRGAN), a cutting-edge deep learning-based image super-resolution technique, is assessed in producing perceptually realistic high-resolution rainfall data over India from the low-resolution input. The main component of SRGAN is a generator network that takes abstract information from low-resolution (LR) rainfall data to infer potential high-resolution (HR) counterparts. A Super-Resolution Residual Neural Network (SRResNet) is used as the generator network. It is trained using a supervised learning strategy (SRResNet) and adversarial learning strategy (several variants created, e.g., SRGAN-MSE, SRGAN-VGGB2, SRGAN-VGGB3 and SRGAN-VGGB4). A statistical downscaling method called bias correction and spatial disaggregation (BCSD) is also employed to compare with the deep learning-based downscaling methods. All these methods are rigorously assessed for their ability to reconstruct distribution, mean, and extreme rainfall during the test period. Our results show that the supervised learning-based SRResNet and adversarial learning-based SRGAN-MSE variant has an upper hand over the BCSD method for gridded rainfall downscaling. These findings have important implications for enhancing the precision and quality of regional climate data in the context of climate change impact assessment.

Keywords Downscaling · Climate data · Gridded rainfall · Deep learning · SRGAN · Image super-resolution

Introduction

The changing climate and its impacts are among the foremost challenges of the current century. With high confidence, the Intergovernmental Panel on Climate Change has stated that the exposure and vulnerability of the Asian population to climate change will increase in the future (IPCC 2022). This elevates the requirement for improving the regional scale climate change studies over Asia. Data is the fuel for scientific understanding, and high-resolution climate datasets for the future timescale are a requirement to understand the spatiotemporal evolution of potential climate change impacts and to implement adequate adaptation and mitigation strategies in advance. In general, Earth System Models (ESM) and Global Climate Models (GCM), which are typically global simulations at coarse resolution, offer crucial insights into the future climate (Taylor et al. 2012; Eyring et al. 2016). However, they are not necessarily optimal for studies of regional climate due to coarse resolution and lack of representation of regional dynamics and sub-grid scale processes (Kumar et al. 2013, 2022). Regional climate change studies and investigations require high-resolution, high-quality datasets, and the solution is to downscale the coarse data.

Downscaling is the process of increasing the horizontal resolution of gridded climate data via dynamical or statistical downscaling methods. Dynamical downscaling is an initial/boundary value problem in which a regional model takes in the initial and boundary conditions from ESM/GCM simulations and numerically resolves them to generate high-resolution data over a limited area (Giorgi and Gao 2018). This method is computationally intensive but scientifically

✉ Pankaj Kumar
kumarp@iiserb.ac.in

[1] Department of Earth and Environmental Sciences, Indian Institute of Science Education and Research, Bhopal, India

proven and adapted for regional climate studies across the globe (Jacob et al. 2012). On the other end, the statistical downscaling methods are computationally cheaper to implement and involve mostly data-driven methods. Due to the availability of powerful computing resources and large-scale datasets, data-driven approaches like artificial intelligence, machine learning, and deep learning (AI/ML/DL) techniques have expanded significantly in recent years (LeCun et al. 2015). This opens a wide range of opportunities to improve the existing climate modeling framework and to generate high-quality, high-resolution climate datasets at a cheaper computation cost.

Reichstein et al. (2019) draw an analogy between deep learning-based single-image super-resolution and spatial downscaling of gridded climate data. Surrounding this idea, there have been multiple recent studies targeted to develop AI/ML/DL-based techniques for the downscaling of climatic variables. A major advancement of image super-resolution-based precipitation downscaling is DeepSD, in which a stacked super-resolution convolutional neural network was trained to map low-resolution precipitation data to high-resolution over the continental United States (Vandal et al. 2018). Sachindra et al. (2018) used machine learning techniques like support vector machine, relevance vector machine and artificial neural networks to downscale precipitation data from 48 precipitation observation stations located across Victoria, Australia. A study by Vandal et al. (2019) inter-compared the performance of machine learning methods such as elastic-net, support vector machine, multi-task sparse structure learning and autoencoder neural networks for downscaling precipitation gauge data and reanalysis dataset over the Northeastern United States region. He et al. (2016) introduced a novel machine-learning-based technique, adaptable random forests, for statistical downscaling of precipitation data. Li et al. (2020) investigated the performance of statistical and machine learning methods in developing multi-model ensembles for downscaling long-term daily temperatures. Tran Anh et al. (2019) proposed using long short-term memory and feedforward neural network model architectures for downscaling precipitation data for the Vietnamese Mekong Delta. Sha et al. (2020a, b) employed a UNet model to downscale gridded data, PRISM (2 m Temperature and precipitation). They proposed an enhanced Nest-UNet, by adding a deep-layer aggregation and nested skip connections. Wang et al. (2021) used a deep residual neural network to downscale daily precipitation and temperature over regions in the United States. Cheng et al. (2020b, 2022) applied the super-resolution generative adversarial network named DeepDT to downscale climate prediction to a higher spatial resolution over a small region in China. Several other studies over the recent years have explored the use of different machine learning and deep learning-based data-driven models in downscaling climate data as a potential alternative to conventional statistical and dynamical downscaling (Cheng et al. 2020a; Leinonen et al. (2021); Sun and Lan 2021; Harris et al. 2022; Wang et al. 2021; Rampal et al. 2022; Baño-Medina et al. 2020).

The downscaling of rainfall data is even more challenging due to its skewed distribution and sparse extremes. The socioeconomic conditions in India are largely dependent on the Indian Summer Monsoon and already a few research works have been employed on deep learning-based downscaling of gridded rainfall, focussing on India. Following the methodology of Vandal et al. (2017), Kumar et al. (2021) applied the DeepSD technique over India to downscale IMD gridded rainfall data, producing good results. Harilal et al. (2021) implemented an augmented convolutional long short-term memory network (ConvLSTM) to downscale low-resolution precipitation simulated by an ESM by incorporating various auxiliary variables concatenated to the input to increase the downscaling skill. In a subsequent study, an intercomparison of various novel deep learning techniques for downscaling gridded rainfall over India was conducted by Kumar et al. (2023), in which an SRGAN, ConvLSTM, U-Net and DeepSD, were employed for downscaling IMD gridded rainfall, and concluded that the SRGAN has a better skill over other deep learning methods. Their experiments were based on a synthetic scenario setup, whereas the input LR is derived from the HR data itself. Also, the training and testing of these experiments were confined to a limited period (1979–2009), and an emphasis was given on evaluation at city-scale, in which the SRGAN is reported to be a promising downscaling method.

Generative Adversarial Network (GAN), in general, is an advanced class of deep learning algorithm consisting of two separate deep neural networks; a generator and a discriminator (Goodfellow et al. 2014). The generator tries to generate fake samples out of a given input/noise, while the task of the discriminator is to distinguish the generated samples from the real samples. Therefore, the GANs are trained by the adversary between the generator and the discriminator. Since its inception, various types of GANs have been successfully implemented for several complicated tasks, for example, generating realistic photographs (Karras et al. 2018), image-to-image translation (Isola et al. 2018; Zhu et al. 2020), text-to-image translation (Zhang et al. 2017), video prediction (Vondrick et al. 2016), 3-D object generation (Wu et al. 2017), image super-resolution (Ledig et al. 2017) etc. The SRGAN is particularly trained to enhance the quality of low-resolution images (Ledig et al. 2017). It is optimized by minimizing a custom loss function called perceptual loss, which is based on the pre-trained VGG-19 network. Ledig et al. (2017) showed that SRGAN works well with RGB images.

This study intends to train SRGAN, a cutting-edge deep learning-based image super-resolution technique, for

downscaling and generating high-resolution rainfall maps of India. Apart from previous studies, several variants of SRGAN are delivered by altering the parameters like training strategy and loss functions. Therefore, this study will focus on an in-depth evaluation of the SRGAN technique for gridded rainfall downscaling. These downscaling methods are also compared with a traditional statistical downscaling method called BCSD. Also, a longer period is chosen for model training (1901–1999 JJAS) and testing (2000–2021 JJAS). To summarize, the following bullet points account for the objectives and relevance of the presented study:

- A deep learning-based image super-resolution technique is applied to a climate science application, which is to downscale and reconstruct high-resolution rainfall data.
- A deep residual neural network for image super-resolution tasks is trained with gridded rainfall data sets via supervised and adversarial training strategies.
- Experiments are designed to showcase how a pre-trained network-based perceptual loss enhances/deteriorates the perceptual quality of generated data.
- Quantitative and qualitative assessment of the transferability of a deep-learning technique to climate science application.

Study area and data

This study is conducted over India. Figure 1 displays a topographical map of the study area, utilizing elevation data sourced from the United States Geological Survey Digital Elevation—Global 30 Arc-Second Elevation (USGS-GTOPO30; https://doi.org/10.5066/F7DF6PQS). India is characterized by the Indian summer monsoon rainfall, also known as the Southwest monsoon, during the June-July–August-September (JJAS) months every year. The gridded rainfall data provided by India Meteorological Department (IMD) for 1901–2021 at a daily scale is used for this study. IMD provides this data at $1° \times 1°$ (IMD-LR; Rajeevan et al. 2008) and $0.25° \times 0.25°$ (IMD-HR; Pai et al. 2014). This dataset is prepared by merging rain gauge records. The location of rain gauges as of 2015 is marked with magenta

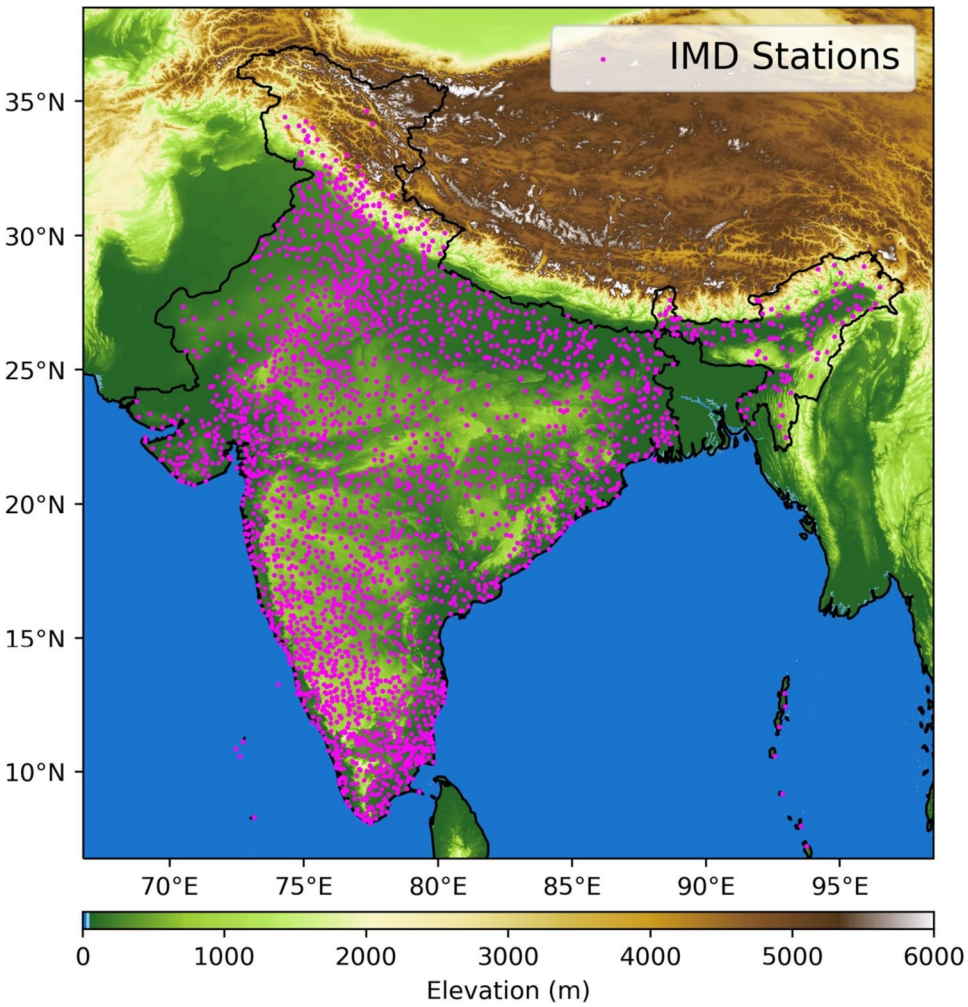

Fig. 1 Elevation map of the study area considered in this study. Elevation data is obtained from USGS-GTOPO30. The magenta dots represent the locations of rain gauges that have contributed to the preparation of the IMD gridded rainfall dataset (Pai et al. 2014)

dots in Fig. 1. Only the monsoon season, i.e., JJAS data, is used for training and testing. The training set is taken as 1901–1999 JJAS (12,078 samples), and the trained models were tested upon data available for 2000–2021 JJAS (2684 samples). Square domains of 128×128 (32×32) grid size are considered for the high-resolution (low-resolution) data expanding over 66.75E-98.5E longitudes and 6.75N-38.5N latitudes. The raw data contains values only within the Indian national boundary, but all unspecified grid points were replaced by zeroes during pre-processing.

Methodology

Network architecture

Two separate deep neural networks, a generator (G) and a discriminator (D) make up the SRGAN. The backbone of the implemented SRGAN is the convolution layers. Convolutional networks are efficient in learning patterns from 2-dimensional datasets such as images. A convolutional kernel of predefined size convolves over the 2-dimensional input array at regular stride intervals by doing element-wise multiplication. The kernel weights and bias are the trainable parameters, and while training, these parameters will be updated via backpropagation (Li et al. 2022). Several such convolutional layers are stacked together to form deep convolutional neural networks (CNNs). One challenge in training deep CNNs is the vanishing/exploding gradient and model performance degradation issues with an increase in network depth. The residual network is proposed as a solution to solve this, which is accomplished by implementing skip connections. The skip-connections are additional connections within a deep CNN apart from the linear connections. The input tensor to a convolution layer or block of layers is element-wise added/concatenated to the layer/block output. Such networks are called residual networks, and they are more immune to vanishing/exploding gradients and degradation issues (Wang et al. 2021). Activation layers are added to the network architecture to incorporate non-linearity into the system. The rectified linear unit (ReLU) activation is used in G as well as D. If x is the input tensor, the mathematical formula for ReLU is

$$f(x) = max(0, x)$$

Figure 2 is the architecture block diagram of SRGAN followed in this study. The G within the SRGAN itself is a super-resolution residual network (SRResNet) primarily built by combining four residual-in-residual dense blocks (RRDB). It is termed RRDB since it has several concurrent skip connections within a single block. The block diagram of SRResNet is given in Fig. 2a. Each RRDB consists of three activation layers, and four 2-dimensional convolution layers, the final of which has a 1×1, and the first three have 3×3 filters. The multiple skip connections within RRDB let them learn and preserve features from training data more effectively (He et al. 2015). Multiple skip connections are maintained by concatenating the layer input and output (Fig. 2a). The RRDB is followed by two upsampling layers where grid points are doubled when passed through each layer. The upsampling layers simply execute the nearest neighbour interpolation and do not contain any learnable parameters. Finally, ReLU activation is applied to all activation layers of the generator network.

The input to the G is low-resolution rainfall data (I_{LR}), and it generates super-resolved rainfall data (I_{SR}) as output. Then the I_{SR} and the true HR label (I_{HR}) is given as input to the discriminator (D). There are several convolution layers at the beginning of the D, where it learns to extract relevant features from the given input (Fig. 2b). The convolution layers are followed by a couple of dense layers, and the output layer at the end has a 'Sigmoid' activation, which provides a probability score between 0 and 1 to convince whether the given input is fake (0) or real (1), respectively. The task of the discriminator network (D) is to give a score, which ascertains whether the input data came from the distribution of real samples (I_{HR}) or generated samples (I_{SR}). As the training progresses, the generator can create more realistic images so that the discriminator may classify them as real.

Training strategies

Supervised training strategy

A neural network contains several trainable parameters. While training a neural network, the objective is to adjust these parameters in the best possible way. The parameters update is done by the optimizer through a backpropagation algorithm. Supervised training is a simple way of training a neural network if a labeled dataset is available. The term labeled dataset means the availability of input-target pairs of data samples. Here, the goal is to predict a target field if an input field is passed into the neural network. In this study, the input field corresponds to the LR data and the target field is the HR data. While training, the neural network's task is to learn the most appropriate mapping between the LR and HR data.

As discussed in the above section, the SRResNet is the neural network architecture we used in the present study. Figure 3a is a diagram showing how supervised training is applied to train the SRResNet with the available input-target pair. The learnable parameters of SRResNet are initialized randomly, and the LR data is passed into the network through the input layer. The SRResNet will then generate HR vaguely, subsequently, the mean squared

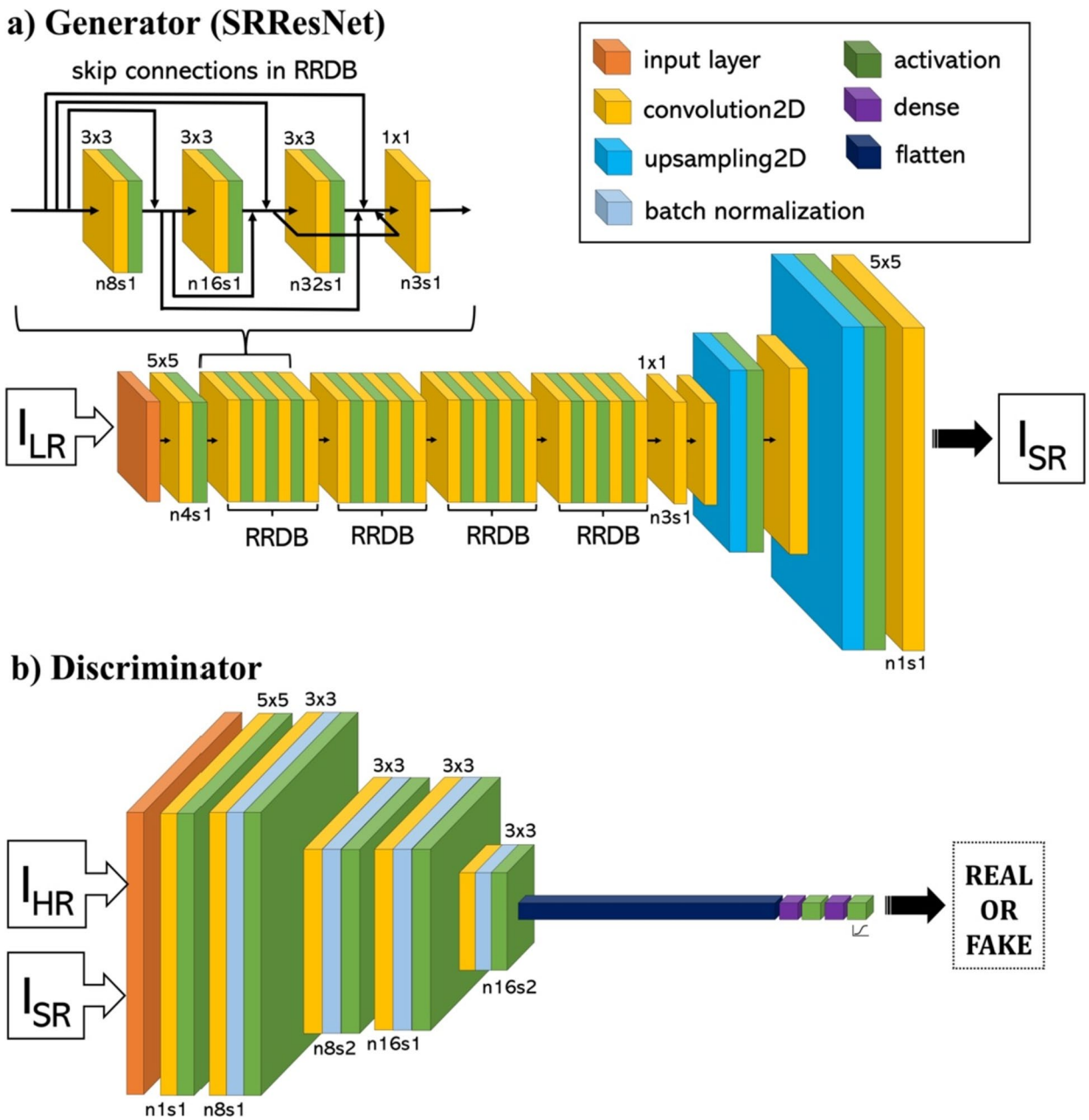

Fig. 2 Architecture of neural networks used in this study. **a** Architecture of SRResNet, which also serves as a generator network of SRGAN; **b** Architecture of discriminator network. The filter size of the convolution layer is mentioned at the top. The number of filters (n) and stride number (s) is given at the bottom of the convolution layer. For example, the label '5×5' on the top and 'n4s1' at the bottom means four filters of size 5×5 convolve with a stride interval of 1

error (MSE) between the generated HR and target HR is calculated. The optimizer will then adjust the trainable parameters in such a way that the MSE is minimized. We used Adam optimizer with learning rate 0.0001 to optimize the SRResNet. This process continues for several iterations until the loss converges. To monitor the SRResNet training, 30% of the entire training samples are kept away from training set for validation. The performance of the SRResNet is validated on the validation dataset to determine how well the model generalizes to unseen scenarios. Once the training is completed, we applied the SRResNet to generate/super-resolve the HR rainfall data for the test period, by providing it with the input LR.

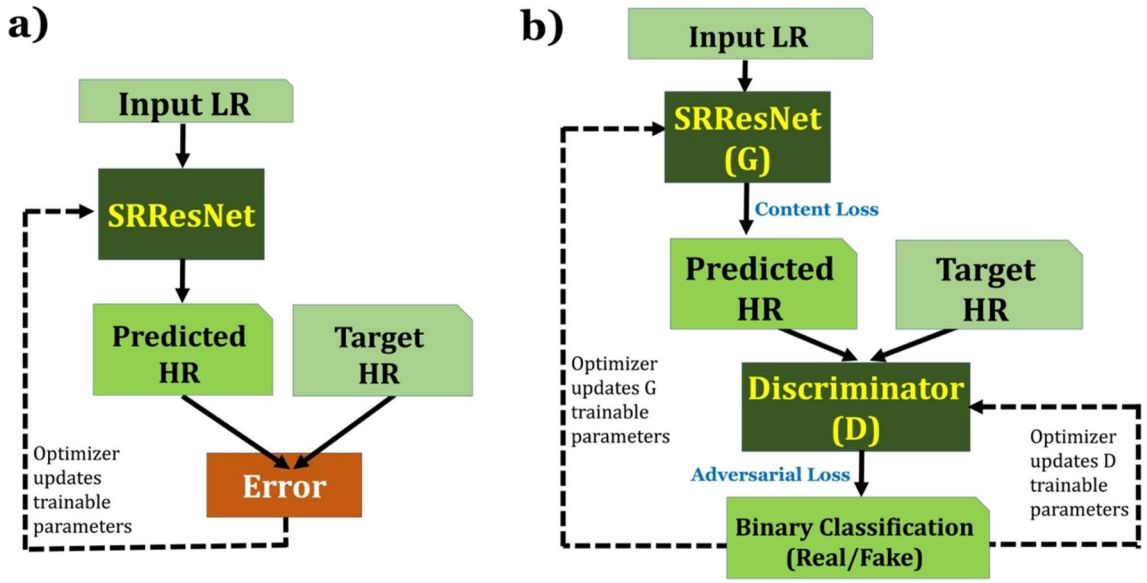

Fig. 3 Training strategies for deep neural networks. **a** supervised training strategy **b** adversarial training strategy

Adversarial training strategy

Adversarial training, also known as the GAN training, is another way to adjust the learning parameters of a deep neural network. It involves an adversarial process where the G and the D are trained simultaneously. Figure 3b is a flowchart showing the steps of adversarial training strategy. G is the SRResNet that generates the HR data and D is a classifier that distinguishes the generated HR and target HR. The G tries to maximize the probability that the discriminator may classify the generated samples as real while the discriminator tries to minimize the same, hence the term adversarial training. The minimax game serves as the pivotal mechanism in Generative Adversarial Network (GAN) training, enabling the accomplishment of intricate and advanced tasks. The fundamental aim is to maintain the training process as a zero-sum game, ensuring equilibrium between the training of the generator (G) and the discriminator (D).

For SRGAN training, a custom loss function called perceptual loss is implemented. Perceptual loss is the weighted sum of content loss from the generator and adversarial loss. The key is the content loss, which is minimized at feature space rather than pixel/grid space. Following the methodology proposed by Ledig et al. (2017), a pre-trained VGG-19 network is used to generate feature maps of both real and generated maps. The content loss is defined as the Euclidean distance between the feature maps created from generated HR as well as target HR.

The content loss (L_{CL}) is defined as the Euclidean distance between the features ($\phi_{i,j}$) from the generated image (I_{SR}) and the actual image (I_{HR}). Therefore,

$$L_{CL(i,j)} = \frac{1}{W_{i,j}H_{i,j}} \sum_{x=1}^{W_{i,j}} \sum_{y=1}^{H_{i,j}} \left(\phi_{i,j}(I_{HR})_{x,y} - \phi_{i,j}(G(I_{LR})_{x,y} \right)^2$$

where $W_{i,j}$ and $H_{i,j}$ are the dimensions of the pretrained VGG-19 generated features. $\phi_{i,j}$ stands for the features generated from ith convolution layer before the jth max pooling layer of the VGG-19 network.

The adversarial loss (L_{AL}) component assists the generator to mislead the discriminator by making realistic samples. It is defined based on the probability of the discriminator over all training samples and is denoted as:

$$L_{AL} = \sum_{n=1}^{N} -logD(G(I_{LR}))$$

So, the overall GAN loss, also termed as perceptual loss (L_{PL}), can be written as:

$$L_{PL} = \alpha.L_{CL} + \beta.L_{AL}$$

where $\alpha = 1$ and $\beta = 10^{-3}$ are the weight coefficients of the respective terms. These coefficients are adopted from Ledig et al. (2017).

In our experiments, the Adam optimizer with a learning rate 0.0001 is applied to optimize the learning parameters of G as well as D.

In a nutshell, the training process of the SRGAN are as follows:

- The SRResNet (G) generates HR samples from an LR input.

- The D receives both the generated HR sample and a real HR sample from the training dataset and evaluates their authenticity.
- The G and the D update their parameters based on their respective loss functions. The generator tries to minimize the loss, which represents the distance between the generated HR and the real HR data, or their feature maps as produced by a pre-trained network. The discriminator tries to maximize the loss, which represents the accuracy of its classifications.
- The training continues until the generator and the discriminator reach an equilibrium, where the generator generates realistic samples that the discriminator cannot reliably distinguish from the real data.
- Upon reaching this equilibrium, the SRResNet (G) is separated and is tested upon the testing set.

Bias correction and spatial disaggregation

To robustly evaluate the trained neural network models for downscaling, we also employed the bias-correction and spatial disaggregation (BCSD) downscaling method (Wood et al. 2002). BCSD is a simple and effective statistical downscaling method widely used by climatologists and hydrologists (Abatzoglou and Brown 2012; Bürger et al. 2012; Maurer and Hidalgo 2008; Maurer et al. 2010; Vandal et al. 2019; Wood et al. 2004). We followed same methodology as Vandal et al. (2019) demonstrated for downscaling gridded precipitation at a daily temporal scale. BCSD consists of two stages: the bias correction of precipitation data using quantile mapping to remove systematic biases and the spatial disaggregation of bias-corrected data to match the fine-scale spatial patterns. For a detailed description of the BCSD deployed in this study, refer to Vandal et al. (2019).

Description of downscaling experiments

Both supervised and adversarial learning strategies are used to train the SRResNet. The description of the experiments conducted are given in Table 1. The BCSD downscaling is deployed as a reference statistical downscaling method, in order to evaluate other methods evaluated in this study. Initially, the SRResNet is trained by supervised training strategy along with validation split to confirm the SRResNet was not overfitting to the training set. Overfitting occurs when the model fits immensely to the training samples but performs weakly on unseen samples.

The SRGAN experiments are designed to evaluate the impact of perceptual loss implementation for training. On the same note, four variants of the SRGAN variants were designed and they are named as SRGAN-MSE, SRGAN-VGGB2, SRGAN-VGGB3 and SRGAN-VGGB4. The SRGAN-MSE does not involve feature extraction while computing the content loss, instead the MSE between generated and target HR is considered. What makes the SRGAN special is the calculation of MSE at feature space rather than pixel space. We used the pretrained VGG-19 network to extract feature maps from the generated HR and target HR. Figure 4a shows the feature extraction steps. The VGG-19 is a deep convolutional classifier network trained on ~ 10 million labeled images from 'IMAGENET' database (Simonyan and Zisserman 2015). It has five blocks of fully connected convolutional layers, followed by dense layers and 'SoftMax' activation at the output layer. Since it has been trained on a wide range of image classes, its potential to retrieve valid feature maps out of a given input is being exploited by implementing the VGG-19-based perceptual loss.

Only the top-level convolutional blocks of VGG-19 (Fig. 4b) are required for feature extraction. Three VGG experiments (SRGAN-VGGB2, SRGAN-VGGB3 and SRGAN-VGGB4) were designed, based on the layer of the pre-trained VGG-19 network from which the features

Table 1 Description of downscaling experiments conducted in this study

Experiment (Model)	Description	Hyperparameters & Specifics
BCSD	Bias correction and spatial disaggregation	
SRResNet	The generator network is trained stand-alone in supervised training mode. Optimized by minimizing the MSE loss function	Learning rate = 0.0001, Batch size = 64, 30% Validation split
SRGAN-MSE	Adversarial training. Content loss is MSE loss between generated and real HR. No feature extraction involved	Trained on batches of batch size 64, Learning rate = 0.0001
SRGAN-VGGB2	Adversarial training. Content loss optimized at high-level features generated from VGG-19 *block2_conv2* layer	
SRGAN-VGGB3	Adversarial training. Content loss optimized at intermediate-level features generated from VGG-19 *block3_conv4* layer	
SRGAN-VGGB4	Adversarial training. Content loss optimized at low-level features generated from VGG-19 *block4_conv4* layer	

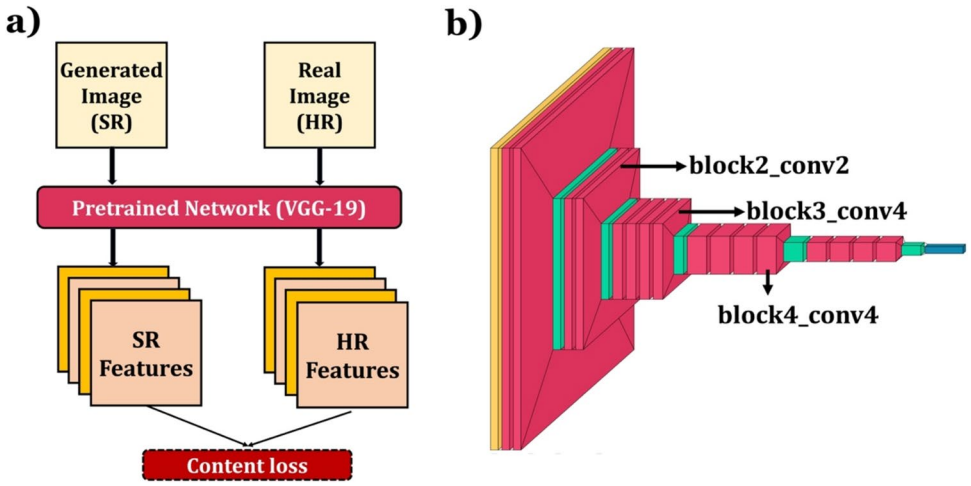

Fig. 4 **a** Flowchart showing feature extraction from a pre-trained network. **b** Architecture block diagram of pre-trained VGG-19 network

are being extracted (Fig. 4b). A detailed description of all experiments conducted is given in Table 1. High-level (*block2_conv2*), intermediate level (*block3_conv4*) and low-level (*block4_conv4*) feature maps produced by specific layers of the pre-trained VGG-19 network were the subjects of experiments.

Evaluation metrics

For the evaluation of trained neural network models, we choose the following metrics:

(i) Root Mean Squared Error (RMSE):

$$RMSE = \sqrt{\frac{\sum_{i=1}^{N}\left(O_i - M_i\right)^2}{N}}$$

(ii) Mean Absolute Error (MAE):

$$MAE = \frac{\sum_{i=1}^{N}\left|O_i - M_i\right|}{N}$$

(iii) Percentage Bias (PBIAS):

$$PBIAS = 100 \times \frac{\sum_{i=1}^{N}\left(M_i - O_i\right)}{\sum_{i=1}^{N} O_i}$$

(iv) Pearson Correlation Coefficient (*CC*):

$$CC = \frac{\sum_{i=1}^{N}\left(O_i - \overline{O}\right)\left(M_i - \overline{M}\right)}{\sqrt{\sum_{i=1}^{N}\left(O_i - \overline{O}\right)^2 \sum_{i=1}^{N}\left(M_i - \overline{M}\right)^2}}$$

where, O_i is the actual observation value, M_i is the model predicted value, N is the total number of non-missing data points, $\overline{O}$ and $\overline{M}$ are the mean of all values of O_i and M_i, respectively.

In addition, to quantify the bias associated with various precipitation rates, we calculated the conditional bias (CB) as the ratio of the mean model predicted precipitation to the mean observed precipitation within each category. The various precipitation categories based on precipitation rate as defined by IMD is provided in Table 2 (Barde et al. 2020). The mathematical notation for CB can be expressed as follows.

For a given precipitation category bounded by lower bound value and upper bound value:

$$CB = \frac{1}{N}\sum_{i=1}^{N}\frac{M_i}{O_i}$$

where, N is the number of data points, M_i is the model predicted precipitation value, and O_i is the model observed precipitation value, in the rainfall category under consideration.

Table 2 Various categories of rainfall events and respective rainfall intensity ranges as defined by India Meteorological Department (IMD)

Description term used	Rainfall amount (mm/day)
Very light rain (VLR)	0.1–2.4
Light rain (LR)	2.5–7.5
Moderate rain (MR)	7.6–35.5
Rather heavy rain (RHR)	35.6–64.4
Heavy rain (HR)	64.5–124.4
Very heavy rain (VHR)	124.5–244.4
Extremely heavy rain (EHR)	> 244.5

Table 3 Performance metrics such as RMSE (mm/day), MAE (mm/day), PBIAS (%) and Pearson's correlation coefficient (CC) of the trained models, calculated aggregately over India

Downscaling method	CC	RMSE	MAE	PBIAS
BCSD	0.601	13.659	5.834	−3.106
SRResNet	0.657	12.25	5.399	−8.418
SRGAN-MSE	0.647	12.373	5.444	−10.005
SRGAN-VGGB2	0.603	13.28	5.448	−46.169
SRGAN-VGGB3	0.541	14.441	6.245	−23
SRGAN-VGGB4	0.539	14.218	6.086	−29.083

Table 4 Performance metrics such as RMSE (mm/day), MAE (mm/day), PBIAS (%) and Pearson's correlation coefficient (CC) of the trained models, calculated aggregately over the Monsoon Core Zone (MCZ)

Downscaling method	CC	RMSE	MAE	PBIAS
BCSD	0.66	11.836	5.141	−0.613
SRResNet	0.699	10.939	4.863	−3.579
SRGAN-MSE	0.694	11.008	4.883	−5.447
SRGAN-VGGB2	0.638	12.158	4.995	−48.929
SRGAN-VGGB3	0.588	12.97	5.631	−22.678
SRGAN-VGGB4	0.588	12.796	5.564	−24.301

Results

The neural network models are trained using the training data set, i.e., 1901–1999 JJAS. Then, the trained models were tested upon the testing set (2000–2021 JJAS). The data for the test period was not exposed while training, and whatever the trained models generate is purely based on what they learned during the training phase. The training curves obtained during the process and the best model selection criteria are described in supplementary information (Figure S1–S5). In addition, the BCSD method was also deployed for downscaling the gridded rainfall data. This section presents an evaluation of the downscaled and reconstructed data by comparing it with the actual IMD-HR for the test period (2000–2021 JJAS).

Overall agreement

The objective metrics such as CC, RMSE, MAE, and PBIAS are calculated to evaluate the reconstructed data. These metrics are calculated aggregately after flattening the entire data array (Tables 3, 4) and are significant at 95% confidence. The CC of each grid point with respect to timesteps is calculated and visualised as a spatial map in Fig. 5. Figure 5 shows that all the downscaled data lack agreement over certain regions, such as mountainous regions (North Himalayas and North-east hills) and rain-shadow regions (Southern Indian peninsula, especially the Tamil Nadu state). The IMD gridded rainfall is derived from rain gauge records only, and the rain gauge density significantly affects its quality over the mountainous regions. This explains the weak correlation over mountainous regions since those areas have sparse rain gauge stations. During JJAS months, the southwest monsoon precipitates mainly over the Western Ghats (WG) and Central India (CI). However, the eastern coasts and Tamil Nadu receive peak rainfall during the northeast monsoon during October–November (Rajeevan et al. 2012), leading to a reduced correlation over rain shadow regions during JJAS. In Fig. 5, it is clear that all grid points covering the WG and CI have a reasonable correlation (>0.6), and the same pattern has also been visible in the reconstructed data by BCSD, SRResNet, SRGAN-MSE, SRGAN-VGGB2, SRGAN-VGGB3 and SRGAN-VGGB4.

Table 2 shows the objective metrics of all methods experimented in this study over India. SRResNet has the minimum RMSE (12.25 mm/day) and maximum correlation (0.657). All methods are observed to have negative PBIAS. The SRGAN-VGGB2 optimised for content loss contributed by high-level features, was more negatively biased. Comparatively, the performance of SRResNet and SRGAN-MSE was almost similar since both were optimised for MSE loss, the first being in supervised mode and the latter being in adversarial mode. Figure 5 reveals that all the downscaling methods perform better over the region bounded as the Monsoon Core Zone (MCZ).

Consequently, the evaluation metrics were computed explicitly for grid points falling within the MCZ, and these results are detailed in Table 4. Figure 6 presents boxplots revealing the distribution of rainfall rates obtained from IMD-HR data and the other reconstructed data to provide a more comprehensive perspective on the data. Figure 6a illustrates the distribution across India, while Fig. 6b depicts the distribution of rainfall rates solely within the MCZ. Interestingly, the distribution of the reconstructed data shows variations across each downscaling scenario compared to the observed IMD-HR data. Nevertheless, it is worth noting that the distribution of rainfall rates for all of India closely mirrors that of the MCZ, which is the same in the reconstructed data case. This suggests that evaluation focusing on MCZ might give some valuable insights into the overall performance and consistency of the downscaling methods being experimented in this study.

Evaluation on Monsoon Core Zone

The MCZ refers to a specific geographical region across India characterized by a pronounced and crucial influence

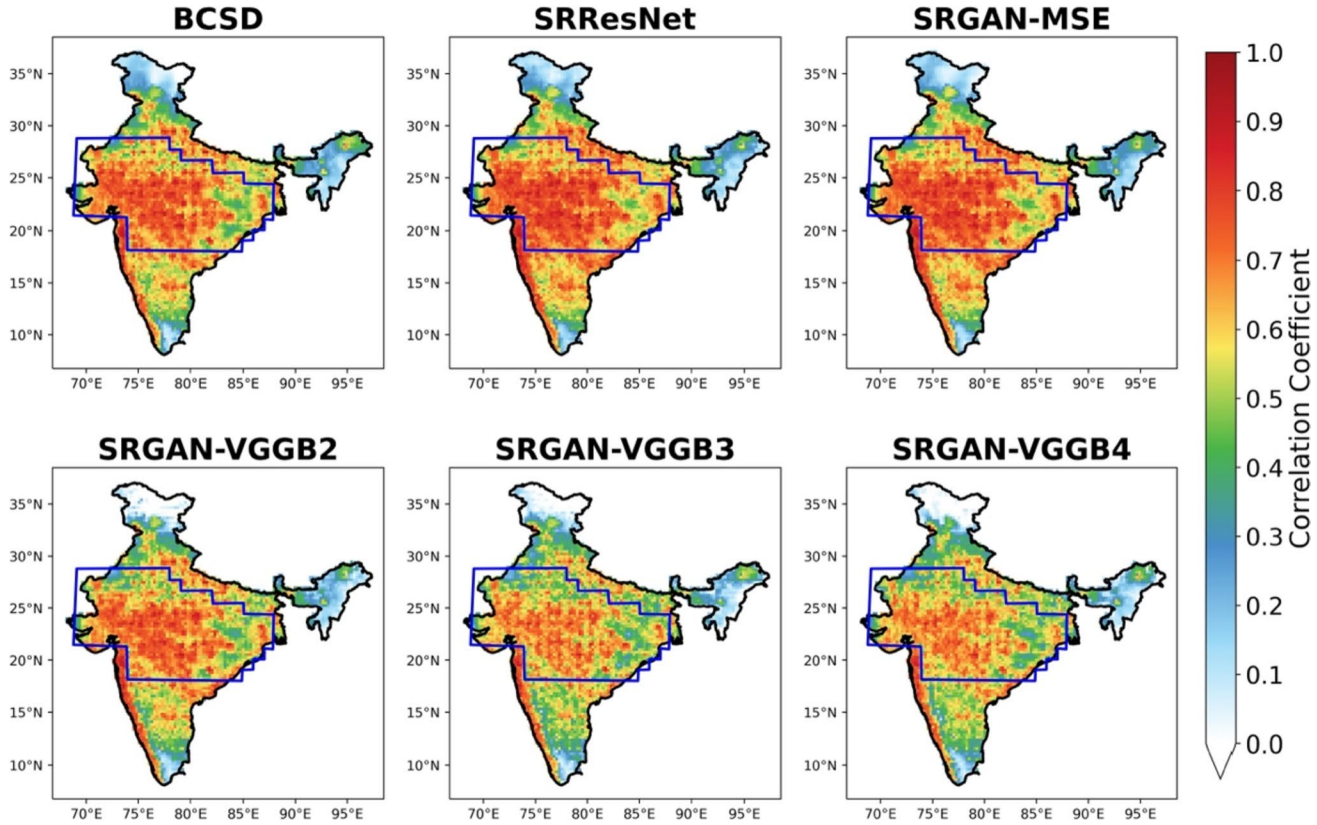

Fig. 5 Spatial map of correlation coefficients (CC) calculated for each grid points of downscaled data from BCSD, SRResNet, SRGAN-MSE, SRGAN-VGGB2, SRGAN-VGGB3 and SRGAN-VGGB4 with IMD-HR during the test period (2000–2021 JJAS). The CC values are significant at 95% confidence interval. The region enclosed within the blue bounding box is the Monsoon Core Zone (MCZ)

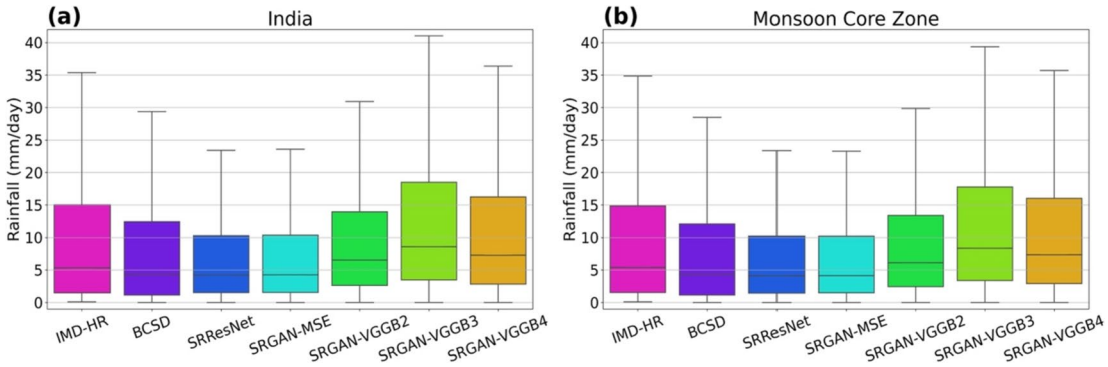

Fig. 6 The boxplots showing the distribution of IMD rainfall data (IMD-HR) and downscaled data by BCSD, SRResNet, SRGAN-MSE, SRGAN-VGGB2, SRGAN-VGGB3, and SRGAN-VGGB4 for **a** entire India and **b** Monsoon Core Zone region

of the Indian summer monsoon (Rajeevan et al. 2006, 2010). This zone is typically situated in central India and experiences distinctive monsoon-related climatic features. This section discusses a detailed evaluation of the downscaling methods based on their performance over MCZ.

The conditional bias (CB) associated with each rainfall category, as described in Table 2, is calculated for the MCZ region and visualized in Fig. 7. These line plots depict CB values relative to rainfall categories, where a CB value of 1 or close to 1 is considered best. Notably, the downscaling methods, including SRResNet, SRGAN-MSE, SRGAN-VGGB2, SRGAN-VGGB3, and SRGAN-VGGB4, exhibit a significant bias due to the overestimation of rainfall values within the very low rain (VLR) category, whereas the BCSD

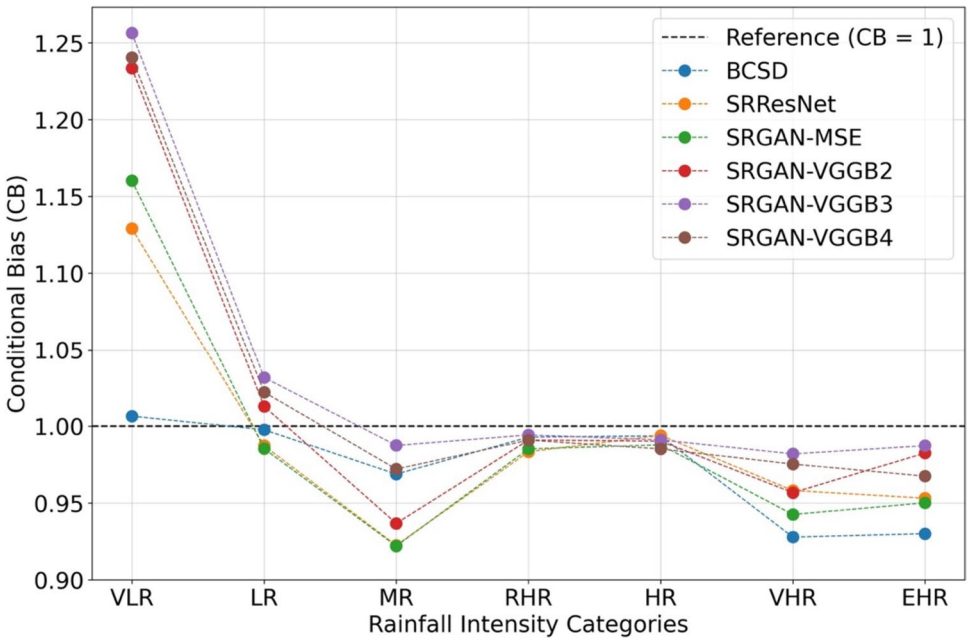

Fig. 7 Conditional bias with respect to various Rainfall Intensity Categories as shown by various downscaling methods followed in this study. The description of the rainfall categories are given in Table 2

method performed the best. However, as traversed to the intense rainfall categories (VHR and EHR), the BCSD is underperforming and other methods, especially the SRGAN-VGGB3 variant, are performing the best. This indicates that the SRGAN variants have better skill in reconstructing high-intensity rainfall events than BCSD.

The variation evaluation metrics such as CC, RMSE, MAE, and PBIAS against percentile are visualized in Fig. 8. These metrics are calculated for events exceeding percentile-based thresholds, which are determined based on field-averaged series over the MCZ. Based on CC, the SRResNet and SRGAN-MSE variants performed better than all other methods across all percentiles ranging from 50 to 99. Noticeably, the CC values are improving for higher percentile events for all methods, with SRGAN-MSE and SRResNet being the best (Fig. 8a). Similarly, based on the RMSE and MAE, SRResNet and SRGAN-MSE are observed to showcase better skills, followed by the BCSD, SRGAN-VGGB2, SRGAN-VGGB3 and SRGAN-VGGB4 variants (Fig. 8b, c). The BCSD method

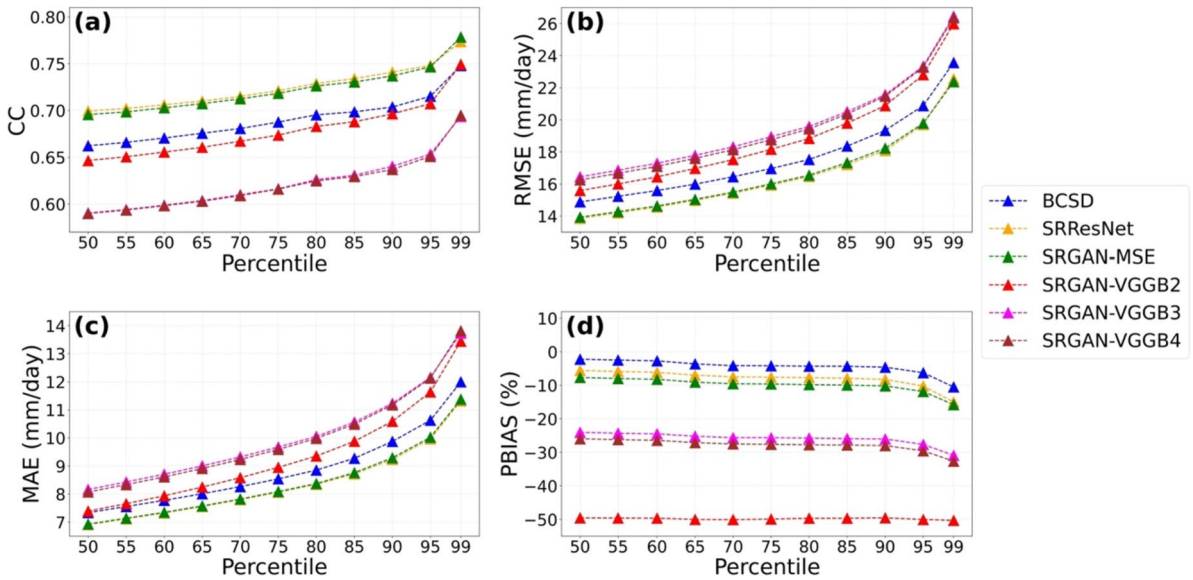

Fig. 8 Variation in performance evaluation metrics, such as **a** correlation coefficients (CC), **b** root mean squared error (RMSE), **c** mean absolute error (MAE), and **d** percentage bias (PBIAS), with respect to percentiles

has lower PBIAS than other methods, which can be attributed to the dedicated bias correction step involved in its preparation (Fig. 8d).

To further our evaluation, we investigated how well the downscaling methods can reconstruct the monthly mean climatology (R) and extremes. We consider two extreme indices to quantify extremes: the 99th percentile magnitude (R99) and maximum 1-day rainfall intensity (Rx1Day). Both are calculated at the monthly frequency for each grid point within MCZ. The error in their reconstruction is calculated as the difference between the reconstructed values from that of the observed, and the spread of error in reconstructed R, R99 and Rx1Day by various downscaling methods are visualized as boxplots in Fig. 9. The error spread of SRResNet and SRGAN-MSE are minimal in reconstructing the R, closely followed by BCSD (Fig. 9a). Regarding extreme indices like R99 and Rx1Day, BCSD and SRGAN-VGGB3 perform better than other methods.

Evaluation on selected samples

The term 'perceptual accuracy' is introduced to describe the precision with which the trained models can identify the grid points of rainfall occurrence in the generated data. Notably, SRGAN training excels in preserving fine details while super-resolving images (Ledig et al. 2017; Kumar et al. 2023). Figure 10 represents four distinct samples drawn from the test set, all falling above the 99th percentile during the test period. SRGAN-VGGB3 and SRGAN-VGGB4 exhibit commendable performance in generating perceptually realistic high-resolution rainfall data, pinpointing the grid points witnessing high-intensity rainfall events. However, their correlation coefficient (CC) values with respect to IMD-HR are relatively low due to persistent negative bias.

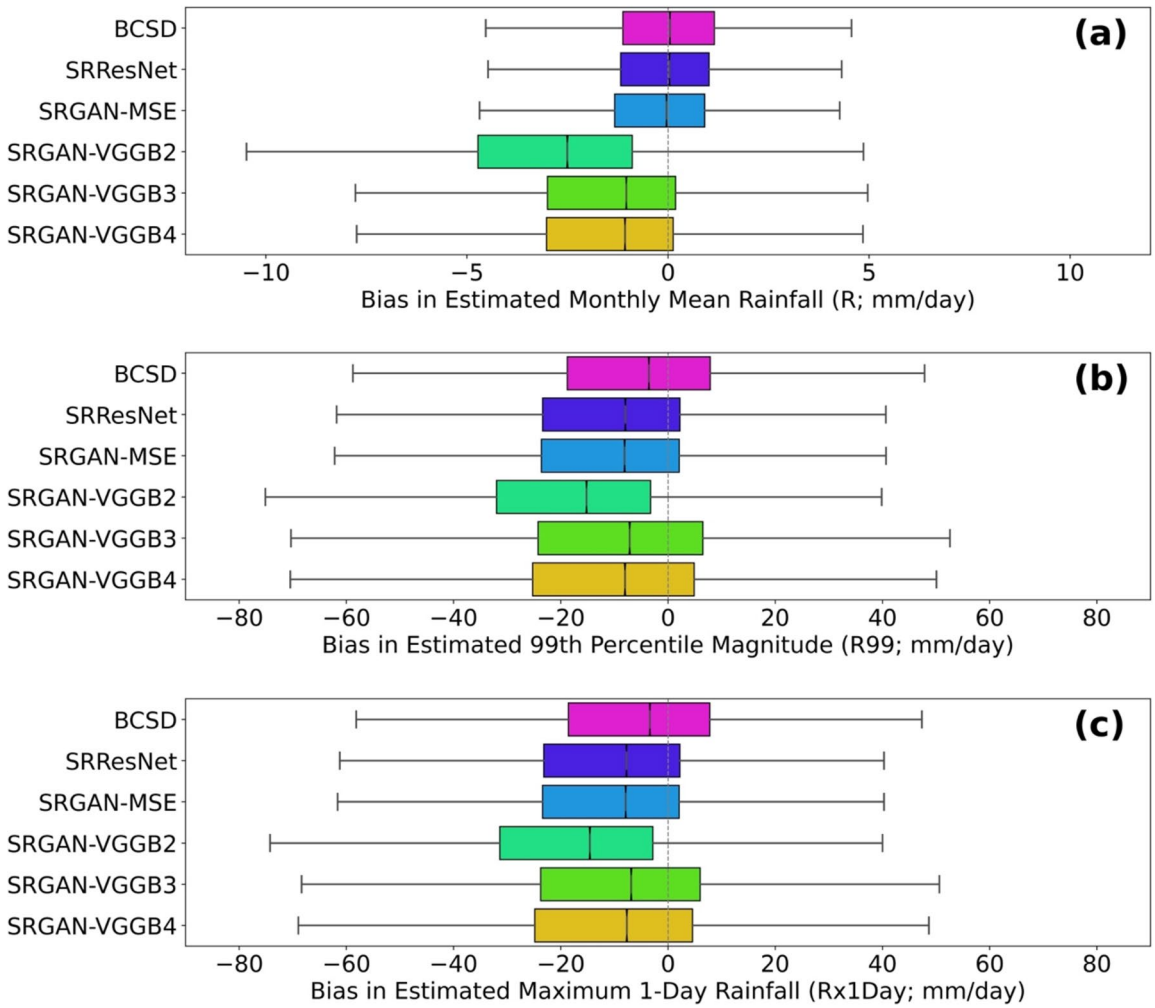

Fig. 9 Boxplots illustrating bias in **a** Estimated mean monthly rainfall, **b** Estimated 99th percentile magnitude at monthly frequency, and **c** Estimated maximum 1-day rainfall for each month, in comparison with IMD-HR during the test period (2000–2021 JJAS)

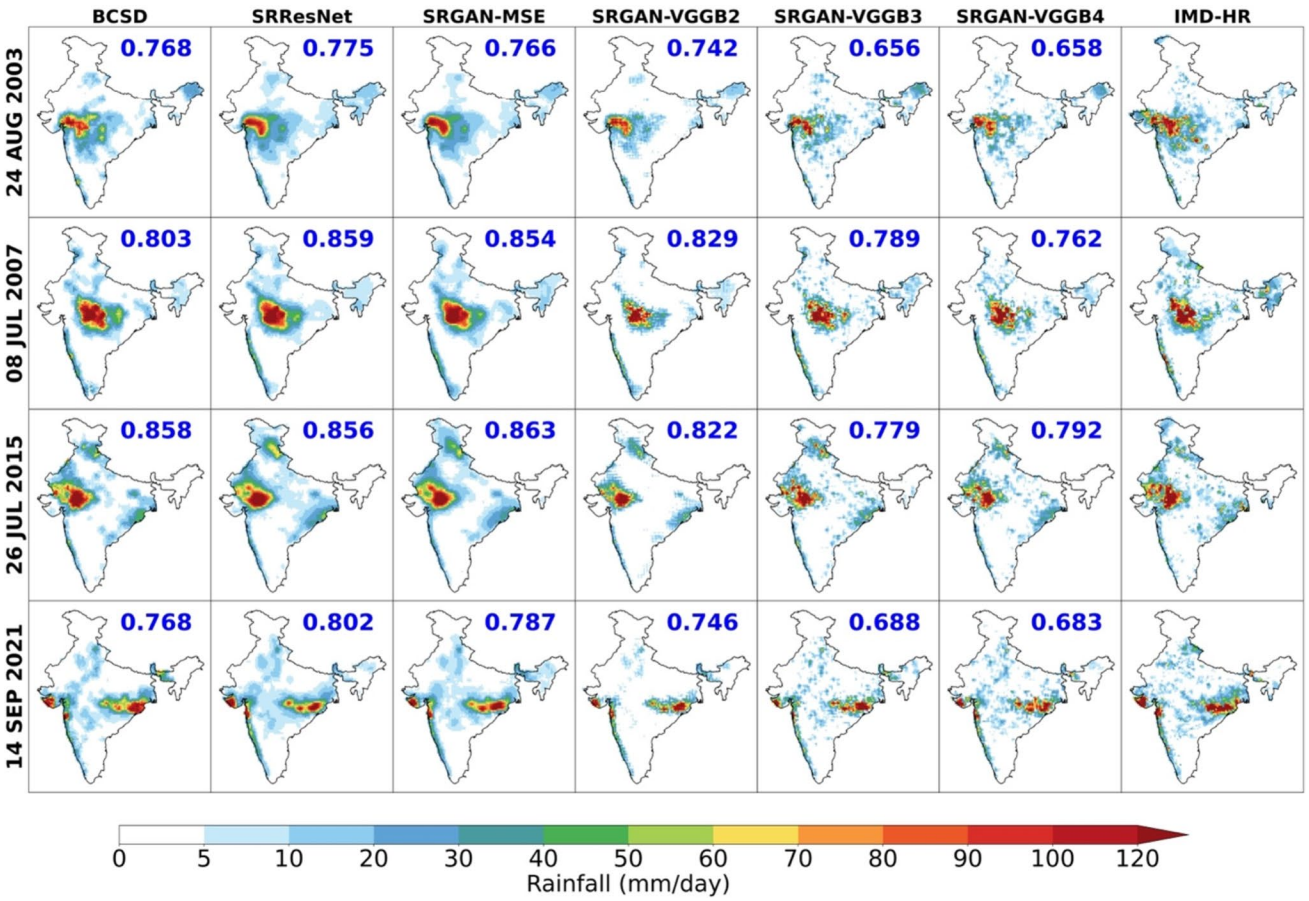

Fig. 10 Examples showing the actual and generated rainfall maps. Each column indicates the downscaling methods. Each row indicates various samples. The correlation coefficient of each sample with respect to IMD-HR is labelled in blue

Conversely, SRGAN-VGGB2 shows unrealistic checkerboard artefacts and tends to underestimate rainfall occurrence. SRResNet and SRGAN-MSE capture the overall data distribution and correlate well with IMD-HR. Nevertheless, the data they reconstruct is overly smoothed and does not accurately pinpoint the exact grid locations of high rainfall intensity. In contrast, SRGAN excels in generating realistic maps that precisely identify grid points of rainfall occurrence, and this consistency is maintained across all time steps within the test period. Figure 11 provides information about the bias in each of these samples as compared with IMD-HR. The reconstructed data by SRResNet and SRGAN-MSE performs on par with or better than the BCSD method. However, the VGG-based variants of SRGAN do not consistently outperform the others, particularly regarding grid points representing low rainfall values.

Discussion

Downscaling rainfall or other variables is an ill-posed problem where a minor input error leads to huge output differences. Rainfall data downscaling is even more challenging due to its stochasticity and highly skewed distribution. This study demonstrated the potential of deep learning techniques to address this problem. Each 1ox1o LR grid point must diffuse into 16 grid points in the four-factor downscaling attempt. The broader objective is to demonstrate the potential, limitations, and transferability of direct implementation of an image super-resolution technique for gridded climate data downscaling. This study also focuses on demonstrating the ability of adversarial learning to preserve minute details while enhancing

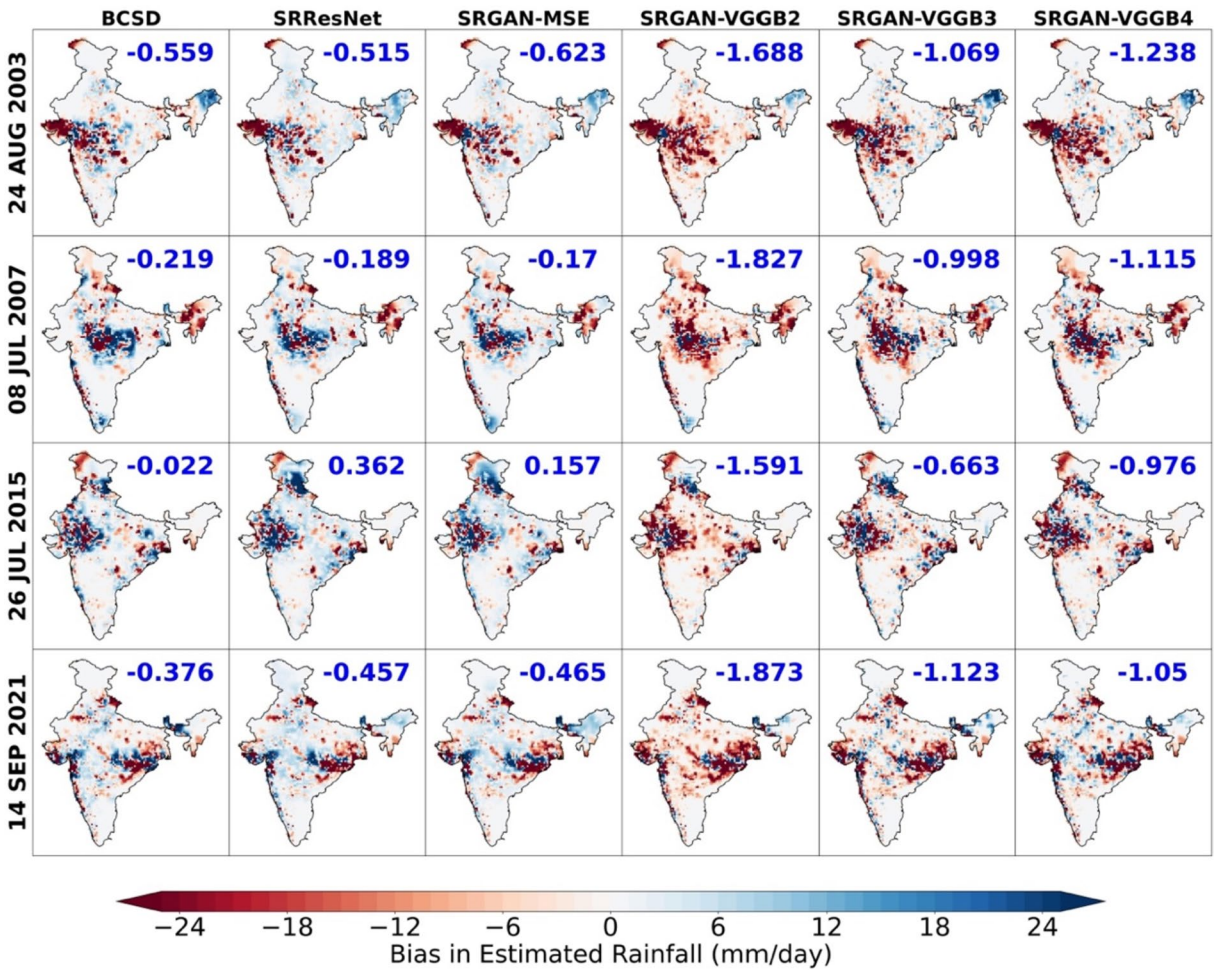

Fig. 11 Bias in selected samples with respect to IMD-HR. The mean bias value over entire grid points is labelled in blue

LR input. Amidst the fact that India is geographically heterogeneous in terms of spatial rainfall distribution, these models are trained to generate rainfall maps of the entire country.

There always exists a trade-off between the resolution of data and the computation requirement to achieve that. If high-resolution data is required, investing more in computation costs is mandatory. However, the novel AI/ML/DL techniques offer an opportunity to generate more realistic data at a cheaper computation cost (Lecun et al. 2015). An extensive change will become possible when such novel techniques can be confidently applied to ESM/GCM data. This study adopts gridded rainfall as a test case since it is a stochastic variable characterized by complex dynamics. Also, this is a non-exhaustive study, and the problem is simplified by limiting the input signal to LR rainfall data only. This study is considered a pure data-driven problem; the trained models are still 'black boxes', and there is room for improvement by various means such as rigorous data cleaning, hyperparameter tuning, restructuring the generator architecture, and augmenting more input variables. (Kashinath et al. 2021; McGovern et al. 2019).

Although DL models are complex to train, they are computationally faster and cheaper during deployment (Vandal et al. 2019). They are faster in computation than dynamical models and may perform better than traditional statistical methods. The scope of this study is to enrich a new class of downscaling methods based on AI/ML/DL techniques that are superior to traditional statistical methods and as effective as dynamical models. The presented results demonstrate the advantages and limitations of the SRGAN technique when directly applied to gridded climate data.

Summary and conclusions

The primary aim of this study is to implement a state-of-the-art image super-resolution technique to downscale and reconstruct high-resolution rainfall data over India. The attempt is to train neural network models that can downscale

IMD gridded rainfall by a factor of four, i.e., $1° \times 1°$ LR data to its $0.25° \times 0.25°$ HR counterpart. Building LR-HR statistical relationships and downscaling according to that will produce smoothened data. One of the observations is that the objective metrics do not accurately reflect the perceptual quality of the data generated by trained SRGAN models. Based on RMSE and correlation, SRResNet was the best, but the generated maps were oversmoothed and unrealistic. The SRResNet and SRGAN-MSE try to minimize the pixel-wise error between generated HR and actual HR, whereas VGG-19-based SRGAN minimizes the MSE at feature space.

The spatial correlation map showed that the downscaling methods have improved skills over the MCZ (Fig. 6). Hence, the evaluation domain is narrowed to MCZ and the conditional bias associated with various intensity-based rainfall categories are investigated (Fig. 7). All downscaling methods, except BCSD, overestimated the low rainfall events, showing a significant bias in lower rainfall rates. However, with very or extremely high rainfall categories, SRGAN variants had the least bias compared to BCSD. The SRResNet and SRGAN-MSE methods outperformed BCSD, but the VGG-based variants of SRGAN were underperforming in most of the evaluation scenario in terms of objective metrics (Fig. 8).

To understand the perceptual similarity of the generated data compared to IMD-HR, an evaluation was carried out on selected samples, which are extreme events falling above the 99th percentile threshold. The VGG-based SRGAN variants, particularly SRGAN-VGGB3, demonstrated a potential to preserve the perceptual quality to a certain extent but failed to reconstruct the magnitude (Figs. 10–11). The spatial difference plots of these selected samples with IMD-HR revealed that the SRGAN-VGGB2, SRGAN-VGGB3, and SRGAN-VGGB4 vastly underestimated the low rainfall values, showcasing deteriorated performance overall. Conversely, the SRResNet and SRGAN-MSE performed better than other methods, as visible in most of our evaluation strategies. In summary, the VGG-based SRGAN variants has limitation in reproducing the exact magnitude of rainfall rate, especially at low rainfall category. But the day wise rainfall maps reconstructed are perceptually similar pinpointing the grid points witnessing high-intensity rainfall events. With further refinements, these deep learning-based downscaling methods could be a potential alternative to traditional statistical methods for gridded rainfall downscaling.

Supplementary Information The online version contains supplementary material available at https://doi.org/10.1007/s40808-023-01899-9.

Acknowledgements The support and the resources provided by PARAM Shivay Facility under the National Supercomputing Mission, Government of India at the Indian Institute of Technology, Varanasi, are gratefully acknowledged.

Author contributions MM Conceptualization, Methodology, Formal analysis, Software, Visualization, Validation, Writing—Original draft preparation—Reviewing and Editing, SG Formal analysis, Software, Writing—Editing PK Conceptualization, Supervision, Funding acquisition, Writing—Reviewing and Editing.

Funding MM received funding for PhD research under the Prime Minister's Research Fellowship (PMRF ID: 0401083) scheme of the Ministry of Education, Government of India. PK received funding from Science and Engineering Research Board, Department of Science and Technology, Government of India, Grant No. CRG/2021/001227.

Data availability The IMD data used in this article is available through the link https://cdsp.imdpune.gov.in/.

Code availability The codes and generated data used for the analysis and plots in this article are available at Figshare via https://doi.org/10.6084/m9.figshare.22110011.v1 with CC0 license.

Declarations

Conflict of interest On behalf of all authors, the corresponding author states that there is no conflict of interest.

Ethical approval Not applicable.

Consent to participate Not applicable.

Consent for publication Not applicable.

References

Abatzoglou JT, Brown TJ (2012) A comparison of statistical downscaling methods suited for wildfire applications. Int J Climatol 32(5):772–780. https://doi.org/10.1002/joc.2312

Baño-Medina J, Manzanas R, Gutiérrez JM (2020) Configuration and intercomparison of deep learning neural models for statistical downscaling. Geosci Model Dev 13(4):2109–2124. https://doi.org/10.1002/joc.2312

Barde V, Nageswararao MM, Mohanty UC, Panda RK, Ramadas M (2020) Characteristics of southwest summer monsoon rainfall events over East India. Theoret Appl Climatol 141(3):1511–1528. https://doi.org/10.1007/s00704-020-03251-y

Bürger G, Murdock TQ, Werner AT, Sobie SR, Cannon AJ (2012) Downscaling extremes—an intercomparison of multiple statistical methods for present climate. J Clim 25(12):4366–4388. https://doi.org/10.1175/JCLI-D-11-00408.1

Cheng J, Kuang Q, Shen C, Liu J, Tan X, Liu W (2020a) ResLap: generating high-resolution climate prediction through image super-resolution. IEEE Access 8:39623–39634. https://doi.org/10.1109/ACCESS.2020.2974785

Cheng J, Liu J, Xu Z, Shen C, Kuang Q (2020b) Generating high-resolution climate prediction through generative adversarial network. Procedia Comput Sci 174:123–127. https://doi.org/10.1016/j.procs.2020.06.067

Cheng J, Liu J, Kuang Q, Xu Z, Shen C, Liu W, Zhou K (2022) DeepDT: generative adversarial network for high-resolution climate prediction. IEEE Geosci Remote Sens Lett 19:1–5. https://doi.org/10.1109/LGRS.2020.3041760

Eyring V, Bony S, Meehl GA, Senior CA, Stevens B, Stouffer RJ, Taylor KE (2016) Overview of the coupled model intercomparison project phase 6 (CMIP6) experimental design and organization.

Geosci Model Dev 9(5):1937–1958. https://doi.org/10.5194/gmd-9-1937-2016
Giorgi F, Gao X-J (2018) Regional earth system modeling: review and future directions. Atmos Ocean Sci Lett 11(2):189–197. https://doi.org/10.1080/16742834.2018.1452520
Goodfellow IJ, Pouget-Abadie J, Mirza M, Xu B, Warde-Farley D, Ozair S, Courville A, Bengio Y (2014) Generative Adversarial Networks (arXiv:1406.2661). arXiv. http://arxiv.org/abs/1406.2661
Harilal N, Singh M, Bhatia U (2021) Augmented convolutional LSTMs for generation of high-resolution climate change projections. IEEE Access 9:25208–25218. https://doi.org/10.1109/ACCESS.2021.3057500
Harris L, McRae ATT, Chantry M, Dueben PD, Palmer TN (2022) A generative deep learning approach to stochastic downscaling of precipitation forecasts. J Adv Model Earth Syst. https://doi.org/10.1029/2022ms003120
He K, Zhang X, Ren S, Sun J (2015) Deep residual learning for image recognition (arXiv:1512.03385). arXiv. http://arxiv.org/abs/1512.03385
He X, Chaney NW, Schleiss M, Sheffield J (2016) Spatial downscaling of precipitation using adaptable random forests. Water Resour Res 52(10):8217–8237. https://doi.org/10.1002/2016wr019034
IPCC (2022) Climate change 2022: impacts, adaptation, and vulnerability. In: Pörtner H-O, Roberts DC, Tignor M, Poloczanska ES, Mintenbeck K, Alegría A, Craig M, Langsdorf S, Löschke S, Möller V, Okem A, Rama B (eds) Contribution of working group II to the sixth assessment report of the intergovernmental panel on climate change. Cambridge University Press
Isola P, Zhu J-Y, Zhou T, Efros AA (2018) Image-to-image translation with conditional adversarial networks (arXiv:1611.07004). arXiv. http://arxiv.org/abs/1611.07004
Jacob D, Elizalde A, Haensler A, Hagemann S, Kumar P, Podzun R, Rechid D, Remedio AR, Saeed F, Sieck K, Teichmann C, Wilhelm C (2012) Assessing the transferability of the regional climate model REMO to different COordinated Regional Climate Downscaling EXperiment (CORDEX) regions. Atmosphere 3(1):181–199. https://doi.org/10.3390/atmos3010181
Karras T, Aila T, Laine S, Lehtinen J (2018) Progressive growing of GANs for improved quality, stability, and variation (arXiv:1710.10196). arXiv. http://arxiv.org/abs/1710.10196
Kashinath K, Mustafa M, Albert A, Wu J-L, Jiang C, Esmaeilzadeh S, Azizzadenesheli K, Wang R, Chattopadhyay A, Singh A, Manepalli A, Chirila D, Yu R, Walters R, White B, Xiao H, Tchelepi HA, Marcus P, Anandkumar A, Prabhat. (2021) Physics-informed machine learning: case studies for weather and climate modelling. Philos Trans R Soc a: Math, Phys Eng Sci 379(2194):20200093. https://doi.org/10.1098/rsta.2020.0093
Kumar P, Wiltshire A, Mathison C, Asharaf S, Ahrens B, Lucas-Picher P, Christensen JH, Gobiet A, Saeed F, Hagemann S, Jacob D (2013) Downscaled climate change projections with uncertainty assessment over India using a high resolution multi-model approach. Sci Total Environ 468–469:S18–S30. https://doi.org/10.1016/j.scitotenv.2013.01.051
Kumar B, Chattopadhyay R, Singh M, Chaudhari N, Kodari K, Barve A (2021) Deep learning–based downscaling of summer monsoon rainfall data over Indian region. Theoret Appl Climatol 143(3–4):1145–1156. https://doi.org/10.1007/s00704-020-03489-6
Kumar P, Mishra AK, Dubey AK, Javed A, Saharwardi MdS, Kumari A, Sachan D, Cabos W, Jacob D, Sein DV (2022) Regional earth system modelling framework for CORDEX-SA: an integrated model assessment for Indian summer monsoon rainfall. Clim Dyn. https://doi.org/10.1007/s00382-022-06217-0
Kumar B, Atey K, Singh BB, Chattopadhyay R, Acharya N, Singh M, Nanjundiah RS, Rao SA (2023) On the modern deep learning approaches for precipitation downscaling. Earth Sci Inform 16(2):1459–1472. https://doi.org/10.1007/s12145-023-00970-4
LeCun Y, Bengio Y, Hinton G (2015) Deep learning. Nature 521(7553):436–444. https://doi.org/10.1038/nature14539
Ledig C, Theis L, Huszar F, Caballero J, Cunningham A, Acosta A, Aitken A, Tejani A, Totz J, Wang Z, Shi W (2017) Photo-realistic single image super-resolution using a generative adversarial network (arXiv:1609.04802). arXiv. http://arxiv.org/abs/1609.04802
Leinonen J, Nerini D, Berne A (2021) Stochastic super-resolution for downscaling time-evolving atmospheric fields with a generative adversarial network. IEEE Trans Geosci Remote Sens 59(9):7211–7223. https://doi.org/10.1109/TGRS.2020.3032790
Li X, Li Z, Huang W, Zhou P (2020) Performance of statistical and machine learning ensembles for daily temperature downscaling. Theoret Appl Climatol 140:571–588. https://doi.org/10.1007/s00704-020-03098-3
Li Z, Liu F, Yang W, Peng S, Zhou J (2022) A survey of convolutional neural networks: analysis, applications, and prospects. IEEE Trans Neural Netw Learn Syst 33(12):6999–7019. https://doi.org/10.1109/TNNLS.2021.3084827
Maurer EP, Hidalgo HG (2008) Utility of daily vs. monthly large-scale climate data: an intercomparison of two statistical downscaling methods. Hydrol Earth Syst Sci 12(2):551–563. https://doi.org/10.5194/hess-12-551-2008
Maurer EP, Hidalgo HG, Das T, Dettinger MD, Cayan DR (2010) The utility of daily large-scale climate data in the assessment of climate change impacts on daily streamflow in California. Hydrol Earth Syst Sci 14(6):1125–1138. https://doi.org/10.5194/hess-14-1125-2010
McGovern A, Lagerquist R, Gagne DJ, Jergensen GE, Elmore KL, Homeyer CR, Smith T (2019) Making the black box more transparent: understanding the physical implications of machine learning. Bull Am Meteor Soc 100(11):2175–2199
Pai DS, Rajeevan M, Sreejith OP, Mukhopadhyay B, Satbha NS (2014) Development of a new high spatial resolution (0.25° × 0.25°) long period (1901–2010) daily gridded rainfall data set over India and its comparison with existing data sets over the region. Mausam 65(1):1–18. https://doi.org/10.54302/mausam.v65i1.85
Rajeevan M, Bhate J, Kale JD, Lal B (2006) High resolution daily gridded rainfall data for the Indian region: analysis of break and active monsoon spells. Curr Sci 91(3):296–306
Rajeevan M, Bhate J, Jaswal AK (2008) Analysis of variability and trends of extreme rainfall events over India using 104 years of gridded daily rainfall data. Geophys Res Lett 35(18):L18707. https://doi.org/10.1029/2008GL035143
Rajeevan M, Gadgil S, Bhate J (2010) Active and break spells of the Indian summer monsoon. J Earth Syst Sci 119(3):229–247. https://doi.org/10.1007/s12040-010-0019-4
Rajeevan M, Unnikrishnan CK, Bhate J, Niranjan Kumar K, Sreekala PP (2012) Northeast monsoon over India: variability and prediction. Meteorol Appl 19(2):226–236. https://doi.org/10.1002/met.1322
Rampal N, Gibson PB, Sood A, Stuart S, Fauchereau NC, Brandolino C, Meyers T (2022) High-resolution downscaling with interpretable deep learning: rainfall extremes over New Zealand. Weather Clim Extremes 38:100525. https://doi.org/10.1016/j.wace.2022.100525
Reichstein M, Camps-Valls G, Stevens B, Jung M, Denzler J, Carvalhais N, Prabhat. (2019) Deep learning and process understanding for data-driven Earth system science. Nature 566(7743):195–204. https://doi.org/10.1038/s41586-019-0912-1
Sachindra DA, Ahmed K, Rashid MdM, Shahid S, Perera BJC (2018) Statistical downscaling of precipitation using machine learning techniques. Atmos Res 212:240–258. https://doi.org/10.1016/j.atmosres.2018.05.022

Sha Y, Gagne DJ II, West G, Stull R (2020a) Deep-learning-based gridded downscaling of surface meteorological variables in complex terrain. Part I: daily maximum and minimum 2-m temperature. J Appl Meteorol Climatol 59(12):2057–2073. https://doi.org/10.1175/jamc-d-20-0057.1

Sha Y, Gagne DJ II, West G, Stull R (2020b) Deep-learning-based gridded downscaling of surface meteorological variables in complex terrain. Part II: daily precipitation. J Appl Meteorol Climatol 59(12):2075–2092. https://doi.org/10.1175/jamc-d-20-0058.1

Simonyan K, Zisserman A (2015) Very deep convolutional networks for large-scale image recognition (arXiv:1409.1556). arXiv. http://arxiv.org/abs/1409.1556

Sun L, Lan Y (2021) Statistical downscaling of daily temperature and precipitation over China using deep learning neural models: localization and comparison with other methods. Int J Climatol 41(2):1128–1147. https://doi.org/10.1002/joc.6769

Taylor KE, Stouffer RJ, Meehl GA (2012) An overview of CMIP5 and the experiment design. Bull Am Meteor Soc 93(4):485–498. https://doi.org/10.1175/BAMS-D-11-00094.1

Tran Anh D, Van SP, Dang TD, Hoang LP (2019) Downscaling rainfall using deep learning long short-term memory and feedforward neural network. Int J Climatol 39(10):4170–4188. https://doi.org/10.1002/joc.6066

Vandal T, Kodra E, Ganguly S, Michaelis A, Nemani R, Ganguly AR (2017) DeepSD: generating high resolution climate change projections through single image super-resolution. In: Proceedings of the 23rd ACM SIGKDD international conference on knowledge discovery and data mining, pp 1663–1672. https://doi.org/10.1145/3097983.3098004

Vandal T, Kodra E, Ganguly S, Michaelis A, Nemani R, Ganguly AR (2018) Generating high resolution climate change projections through single image super-resolution: an abridged version. In: Proceedings of the Twenty-Seventh International Joint Conference on Artificial Intelligence, pp 5389–5393. https://doi.org/10.24963/ijcai.2018/759

Vandal T, Kodra E, Ganguly AR (2019) Intercomparison of machine learning methods for statistical downscaling: the case of daily and extreme precipitation. Theoret Appl Climatol 137:557–570. https://doi.org/10.1007/s00704-018-2613-3

Vondrick C, Pirsiavash H, Torralba A (2016) Generating videos with scene dynamics (arXiv:1609.02612). arXiv. http://arxiv.org/abs/1609.02612

Wang F, Tian D, Lowe L, Kalin L, Lehrter J (2021) Deep learning for daily precipitation and temperature downscaling. Water Resour Res 57(4):e2020WR029308. https://doi.org/10.1029/2020wr029308

Wood AW, Maurer EP, Kumar A, Lettenmaier DP (2002) Long-range experimental hydrologic forecasting for the eastern United States. J Geophys Res: Atmos 107(D20):ACL 6-1-ACL 6-15. https://doi.org/10.1029/2001JD000659

Wood AW, Leung LR, Sridhar V, Lettenmaier DP (2004) Hydrologic implications of dynamical and statistical approaches to downscaling climate model outputs. Clim Chang 62(1–3):189–216. https://doi.org/10.1023/B:CLIM.0000013685.99609.9e

Wu J, Zhang C, Xue T, Freeman WT, Tenenbaum JB (2017) Learning a probabilistic latent space of object shapes via 3D generative-adversarial modeling (arXiv:1610.07584). arXiv. http://arxiv.org/abs/1610.07584

Zhang H, Xu T, Li H, Zhang S, Wang X, Huang X, Metaxas D (2017) StackGAN: text to photo-realistic image synthesis with stacked generative adversarial networks (arXiv:1612.03242). arXiv. http://arxiv.org/abs/1612.03242

Zhu J-Y, Park T, Isola P, Efros AA (2020) Unpaired image-to-image translation using cycle-consistent adversarial networks (arXiv:1703.10593). arXiv. http://arxiv.org/abs/1703.10593